Cell Reports
Methods

Report

Rat post-implantation epiblast-derived pluripotent stem cells produce functional germ cells

Graphical abstract

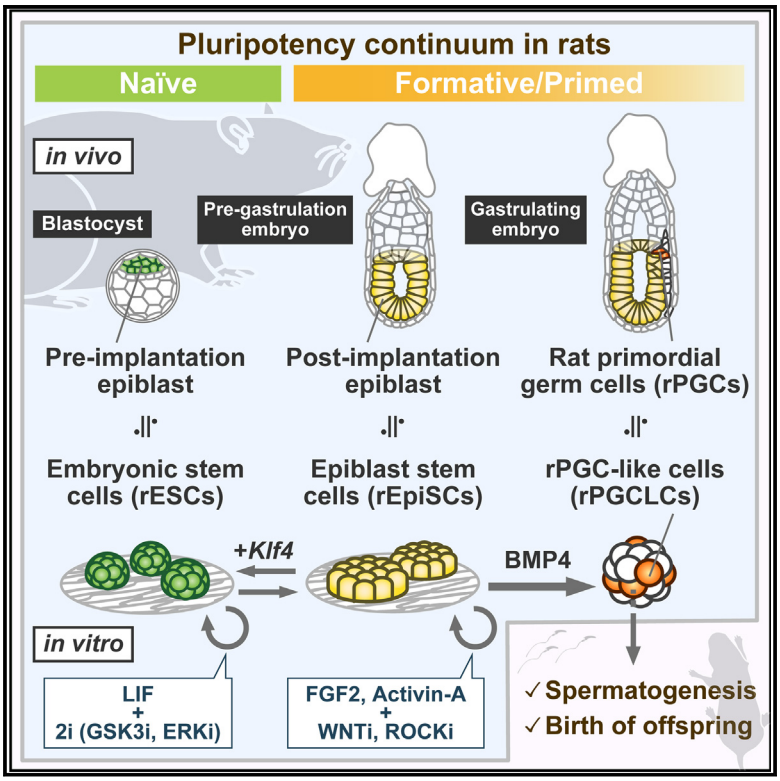

Authors

Kenyu Iwatsuki, Mami Oikawa, Hisato Kobayashi, ..., Kazuki Kurimoto, Masumi Hirabayashi, Toshihiro Kobayashi

Correspondence

tkoba@g.ecc.u-tokyo.ac.jp

In brief

Iwatsuki et al. develop optimal culture conditions for rat epiblast-derived pluripotent stem cells (EpiSCs). These rEpiSCs exhibit molecular similarities to pre-gastrulating pluripotent epiblasts and demonstrate the ability to generate functional germ cells. Therefore, the approach provides valuable tools for studying pluripotency and *in vitro* gametogenesis.

Highlights

- Inhibition of WNT and ROCK is required for uniform and robust expansion of rEpiSCs
- Exogenous Klf4 can reset rEpiSCs into rESC-like cells displaying naive pluripotency
- rEpiSCs can generate rPGCLCs capable of spermatogenesis and giving birth to offspring

Iwatsuki et al., 2023, Cell Reports Methods *3*, 100542
August 28, 2023
https://doi.org/10.1016/j.crmeth.2023.100542

CellPress

Cell Reports Methods

CellPress
OPEN ACCESS

Report

Rat post-implantation epiblast-derived pluripotent stem cells produce functional germ cells

Kenyu Iwatsuki,[1,2] Mami Oikawa,[1,3] Hisato Kobayashi,[4] Christopher A. Penfold,[5,6,7] Makoto Sanbo,[8] Takuya Yamamoto,[9,10,11] Shinichi Hochi,[2,12] Kazuki Kurimoto,[4] Masumi Hirabayashi,[8,13] and Toshihiro Kobayashi[1,8,14,*]

[1]Division of Mammalian Embryology, Center for Stem Cell Biology and Regenerative Medicine, The Institute of Medical Science, The University of Tokyo, Tokyo 108-8639, Japan
[2]Graduate School of Medicine, Science and Technology, Shinshu University, Nagano 386-8567, Japan
[3]Laboratory of Regenerative Medicine, Tokyo University of Pharmacy and Life Sciences, Tokyo 192-0392, Japan
[4]Department of Embryology, Nara Medical University, Nara 634-0813, Japan
[5]Department of Physiology, Development and Neuroscience, University of Cambridge, Downing Site, Cambridge CB2 3EG, UK
[6]Centre for Trophoblast Research, University of Cambridge, Downing Site, Cambridge CB2 3EG, UK
[7]Wellcome Trust – Cancer Research UK Gurdon Institute, Henry Wellcome Building of Cancer and Developmental Biology, University of Cambridge, Tennis Court Road, Cambridge CB2 1QN, UK
[8]Center for Genetic Analysis of Behavior, National Institute for Physiological Sciences, Aichi 444-8787, Japan
[9]Center for iPS Cell Research and Application, Kyoto University, Kyoto 606-8507, Japan
[10]Institute for the Advanced Study of Human Biology (ASHBi), Kyoto University, Kyoto 606-8501, Japan
[11]Medical-risk Avoidance Based on iPS Cells Team, RIKEN Center for Advanced Intelligence Project, Kyoto 606-8501, Japan
[12]Faculty of Textile Science and Technology, Shinshu University, Nagano 386-8567, Japan
[13]The Graduate University of Advanced Studies, Aichi 444-8787, Japan
[14]Lead contact
*Correspondence: tkoba@g.ecc.u-tokyo.ac.jp
https://doi.org/10.1016/j.crmeth.2023.100542

MOTIVATION Pluripotent stem cells (PSCs) that mirror the pluripotent state in the pre-gastrulation epiblast allow us to examine the molecular mechanisms underlying pluripotent transitions and the differentiation of germ line and soma. Despite rats being a prominent animal model for biomedical research, alongside mice, there has been limited investigation into the derivation and characterization of rat PSCs derived from the post-implantation epiblast (rEpiSCs). This study explores the optimal culture conditions for successfully deriving and expanding rEpiSCs. Additionally, we investigate the molecular characteristics of established rEpiSCs, their ability to reset to a naive pluripotent state, and their competence in producing functional germ cells.

SUMMARY

In mammals, pluripotent cells transit through a continuum of distinct molecular and functional states en route to initiating lineage specification. Capturing pluripotent stem cells (PSCs) mirroring *in vivo* pluripotent states provides accessible *in vitro* models to study the pluripotency program and mechanisms underlying lineage restriction. Here, we develop optimal culture conditions to derive and propagate post-implantation epiblast-derived PSCs (EpiSCs) in rats, a valuable model for biomedical research. We show that rat EpiSCs (rEpiSCs) can be reset toward the naive pluripotent state with exogenous *Klf4*, albeit not with the other five candidate genes (*Nanog*, *Klf2*, *Esrrb*, *Tfcp2l1*, and *Tbx3*) effective in mice. Finally, we demonstrate that rat EpiSCs retain competency to produce authentic primordial germ cell-like cells that undergo functional gametogenesis leading to the birth of viable offspring. Our findings in the rat model uncover principles underpinning pluripotency and germline competency across species.

INTRODUCTION

Pluripotent cells, the founding cells of the body, exist transiently in early mammalian embryos and can be captured as pluripotent stem cells (PSCs) *in vitro*. PSCs can expand indefinitely in an undifferentiated state and give rise to all the body cell types in response to various differentiation stimuli. While all PSCs require a unique gene regulatory network consisting

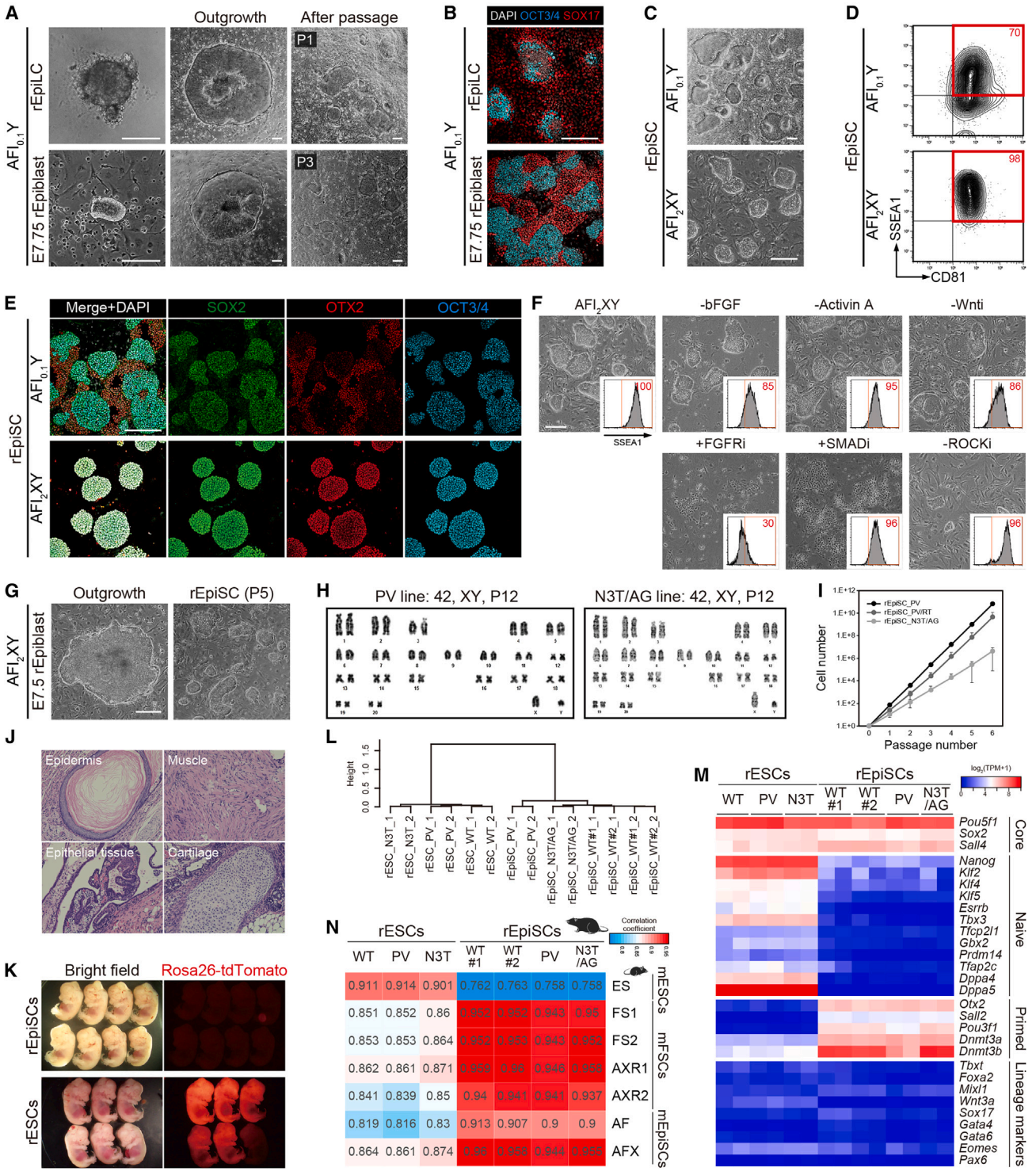

Figure 1. Characterization of rat epiblast stem cells

(A) Morphology of 54-h rEpiLC (top), E7.75 rat epiblast stem cell (rEpiblast) (bottom), and their derivatives on feeder in medium with 20 ng/mL activin-A, 12 ng/mL bFGF, 0.1 μM IWP2, and 5 μM Y27632 ($AFI_{0.1}Y$).

(B) Immunofluorescent (IF) image of rEpiSC derived from rEpiLC and E7.75.

(C) Morphology of rEpiSCs in medium with different concentrations of Wnti: 0.1 μM IWP2 ($AFI_{0.1}Y$) and 2 μM IWP2 and 5 μM XAV939 (AFI_2XY).

(D) FACS pattern of rEpiSCs.

(E) IF of rEpiSCs.

(legend continued on next page)

of core pluripotency factors such as *Oct3/4* and *Sox2* for maintenance, there are several PSCs with molecularly and functionally distinct pluripotent states, mirroring early embryonic development.[1]

"Naive" PSCs with unbiased developmental potential correspond to the pluripotent state of the epiblast in the pre-implantation blastocyst.[2] In rodents, the incorporation of naive PSCs into the ICM via blastocyst injection generates chimeric animals with PSC-derived cells in all the tissues, including the germ line.[3] "Primed" PSCs, poised to initiate lineage-specific programs, reflect features of pluripotent epiblasts at the mid-gastrulating embryonic stage. In mice, epiblast stem cells (EpiSCs) derived from the epiblast at embryonic day (E)5.5–8.0, using fibroblast growth factor (FGF) and activin, are defined as primed PSCs.[4–7] While primed PSCs can readily differentiate into all the somatic lineages, they do not form chimeras upon blastocyst injection, likely due to the discordance between developmental stages of the donor and host cells.[8] Recently, several groups have reported an intermediate pluripotent state between naive and primed, termed "formative," PSCs.[9–11] Formative PSCs are representative of mouse post-implantation epiblasts between E5.5 and E6.0. They can form chimeras upon blastocyst injection at low frequency. A key feature of formative PSCs is their competence to induce primordial germ cell (PGC)-like cells (PGCLCs) *in vitro* in response to the bone morphogenetic protein (BMP) signal. In mice, epiblasts gain germline competency transiently (between E5.5 and E6.5).[12] This state is recapitulated *in vitro* by inducing epiblast-like cells (EpiLCs) from naive PSCs.[13] EpiLCs are heterogeneous and persist only transiently. Thus, formative PSCs can be regarded as self-renewing EpiLCs. These distinct pluripotent states, captured *in vitro*, exist in a continuum and transit along the developmental flow.[14] Furthermore, forced expression of naive pluripotency factor(s) in primed PSCs can reset the transcriptional regulatory network. In addition, specific culture conditions reprogram primed PSCs back to naive PSCs.[15] Thus, capturing unique pluripotent states in culture as expandable cell lines provides a valuable tool to understand the molecular mechanisms underpinning pluripotency transitions, germline/soma fate determination, and cellular reprogramming.

The rat (*Rattus norvegicus*) PSC model, alongside mice, allows the delineation of conserved principles between various pluripotency states. Like in mice, assays using embryo manipulation and reproductive technology are now well established for rats. Therefore, we now have the tools to examine if rat PSCs follow the criteria used to define pluripotent states in mice and humans.[16] In rats, naive PSCs can only be derived in a chemically defined medium with two specific inhibitors (2i) against extracellular signal-regulated kinase (ERK) and glycogen synthase kinase 3 (GSK3) together with leukemia inhibitory factor (LIF) on feeders.[17–19] Even though rats are a valuable biomedical model system, the stringent culture condition requirements for naive PSC derivation delayed the generation of PSC-mediated genetically modified rats by over 25 years relative to mice. However, the derivation and culture of rat PSCs formed the basis for the successful derivation of naive human PSCs,[20–22] exemplifying the importance of the rat model system in bridging the gap between mouse and human models.

Here, we endeavor to derive rat PSCs reflecting the pluripotent state of the post-implantation epiblast. A pioneering study demonstrated the successful derivation of rat EpiSCs (rEpiSCs).[4] However, these rEpiSCs are under-studied and have not been tested for PGCLC competence *in vitro*. Recently, we established an *in vitro* system recapitulating pluripotency transition from naive rat ESCs (rESCs) to formative rat EpiLCs (rEpiLCs) via the formation of spherical aggregates, with efficient rat PGCLC (rPGCLC) induction.[23] This robust *in vitro* system and the methods for functional assessment of rPGCLCs developed by us provide tools to investigate the properties of rEpiSCs.

In this study, we explore culture conditions optimal for derivation and robust expansion of rEpiSCs as a homogenously undifferentiated population. We find that *Klf4*, a naive pluripotency factor, is critical for resetting the gene regulatory network toward naive pluripotency in rats. Surprisingly, none of the other factors shown to reset primed to naive pluripotent network in mice (*Nanog*, *Klf2*, *Esrrb*, *Tfcp2l1*, and *Tbx3*) do so in rEpiSCs. Furthermore, we demonstrate rEpiSCs under our culture conditions do not contribute to chimera formation but retain germline competency to produce PGCLCs leading to live offspring. Therefore, this is the first demonstration of fully functional germ cells induced directly from self-renewable stem cells in mammals.

RESULTS

Derivation of rat epiblast-derived PSCs under defined conditions

First, we sought to identify optimal culture conditions for rEpiSC derivation to investigate their characteristics. Since *in vitro* rESC-derived rEpiLCs are readily produced at scale and accessible for testing multiple culture conditions compared with *in vivo* epiblasts, we used rEpiLCs to optimize conditions for the derivation of rEpiSCs. rEpiLC aggregates were directly harvested on

(F) The effect of each supplement in rEpiSC medium on colony morphology and pluripotency (SSEA1 expression) of rEpiSCs. The rate of SSEA1-positive population represents the mean of three replicates.
(G) Derivation of rEpiSCs from E7.5 rat epiblast in AFI$_2$XY medium.
(H) Karyotype analysis of rEpiSCs using two representative lines at passage 12.
(I) Cell proliferation of rEpiSCs maintained in rEpiSC medium. *Prdm14-H2BVenus* (PV), *PV/Rosa26-tdTomato* (RT), and *Nanos3-tdTomato* (N3T)/*Acrosin-EGFP* (AG) lines show 3 and 4 replicates, respectively, and error bars denote SD.
(J) Hematoxylin and eosin staining of rEpiSC-derived teratomas.
(K) Chimera contribution of rESCs and rEpiSCs. Images show the fetuses at E15.5.
(L) Hierarchical clustering between rESCs and rEpiSCs in several cell lines (wild-type [WT], PV, and N3T/AG lines).
(M) Heatmap of pluripotent genes and lineage marker genes between rESCs and rEpiSCs.
(N) Heatmap of the correlation coefficients among rat PSCs (rESCs, rEpiSCs) and mouse PSCs (ES, FS, AXR, AF, and AFX) from published data.[10]
All scale bars in Figure 1 represent 200 μm.

mitomycin C-treated mouse embryonic fibroblast (MEF) feeder cells (Figure 1A). For the medium, in addition to N2B27 basal medium[24] plus 5% knockout serum replacement (KSR), we added 20 ng/mL activin-A and 12 ng/mL basic fibroblast growth factor (bFGF), used for derivation and maintenance of mouse and rat EpiSCs.[4] We supplemented the medium with 0.1 μM WNT inhibitor (IWP2), a porcupine inhibitor, to prevent spontaneous differentiation and 5–10 μM Rho-associated coiled-coil kinase (ROCK) inhibitor (Y-27632) to support the survival of rEpiSCs, based on our previous study on rabbit PSC derivation.[25] In the culture medium (termed $AFI_{0.1}Y$), rEpiLC aggregates readily attach to the feeder. Subsequently, they formed an epithelial monolayer and proliferated continuously after passage (Figure 1A). However, we detected extensive differentiation as judged by immunofluorescence (IF) staining with pluripotency markers, OCT3/4, and the endoderm differentiation marker, SOX17 (Figure 1B). Similar spontaneous differentiation was also observed in cell lines established from epiblasts isolated from E7.5–7.75 post-implantation rat embryos (Figures 1A and 1B). Since WNT signal induces differentiation in mouse EpiSCs (mEpiSCs),[26–28] we titrated the concentration of its inhibitor. Also, to tightly suppress both WNT secretion and the canonical WNT pathway, we tested the synergistic effect of IWP2 with another WNT inhibitor, XAV-939, a tankyrase inhibitor (Figures S1A and S1B). Then, we standardized an optimal rEpiSC medium composition containing higher doses of two WNT inhibitors (2 μM IWP2 and 5 μM XAV-939). Under the revised culture conditions (hereafter, AFI_2XY) on feeders, epiblast-derived rEpiSCs displayed uniform morphology (Figure 1C) and homogenously expressed OCT3/4, SOX2, and SSEA1 without differentiation (Figures 1D, 1E, and S2C). The rEpiSCs ubiquitously expressed OTX2 and CD81, markers of the post-implantation epiblast (Figures 1D, 1E, and S2C). Activin/nodal or FGF signal inhibition using specific inhibitors in the medium impeded colony formation, confirming their conserved role in proliferation and maintenance of the undifferentiated state like in mEpiSCs and human primed PSCs[29] (Figure 1F). Surprisingly, continuous supplementation of Y-27632 was necessary for the survival of rEpiSCs (Figures 1F and S1C), unlike primed PSCs in other animals (mice, humans, rabbits, pig, sheep, and cow) that require ROCK inhibition only transiently after single-cell dissociation.[25,30,31]

Next, we examined if the AFI_2XY medium is conducive for rEpiSC derivation from epiblasts. We derived rEpiSC lines from E7.5 rat epiblasts in the rEpiSC medium. The isolated epiblasts readily attached to the feeders, and the cultured explant exhibited tightly packed and typical undifferentiated morphology at 2–3 days post harvesting (Figure 1G). After picking colonies, mechanically dissociated clumps formed uniform colonies without any indication of differentiation and were subsequently cultured as rEpiSCs (Figure 1G). The derivation efficiency was 76.2% (32/42 [cell line/epiblast]) in total [cell line/epiblast]). The rEpiSCs were routinely maintained by passaging via single-cell dissociation and stably proliferated, maintaining normal karyotype (Figures 1H and 1I). Further, we tested if the derivation of rEpiSCs was possible from other *in vivo* and *in vitro* sources. We found that rEpiSCs can be obtained from the blastocyst and naive rESCs but take 3–4 days longer to derive than rEpiSCs from the post-implantation epiblast or rEpiLCs, likely due to time required to exit from the naive pluripotent state (Figures S2A and S2B and Table S1). In contrast, only a few cell lines were obtained from E9.5 embryos containing multiple differentiated cell types (Figure S2A and Table S1). Taken together, we conclude that our culture condition is suitable for the derivation of rEpiSCs from the *in vivo* epiblast.

Next, we characterized the rEpiSCs in the culture conditions. Pluripotency-wise, the rEpiSCs could differentiate into three primary germ layers *in vitro* (Figure S2D). After transplantation into the testis of immune-deficient mice, rEpiSCs formed teratoma containing various mature cell types (Figures 1J and S2E). However, we found that rEpiSCs do not contribute to chimera after injection into rat blastocysts (Figure 1K and Table S2). To further characterize rEpiSCs, we examined the transcriptome of multiple rEpiSC lines and compared them with that of naive rESCs with the same genetic background, as indicated in Figure 1L. In hierarchical clustering and correlation heatmap, rEpiSCs and rESCs showed distinct clusters (Figures 1L, S2F, and S2G). Both rEpiSCs and rESCs expressed core pluripotency genes, *Oct3/4* and *Sox2*, at a similar level. rEpiSCs highly expressed some epiblast-specific genes (*Otx2*, *Sall2*, and *Pou3f1*) but not naive pluripotency genes (*Nanog*, *Klf2*, *Klf4*, *Esrrb*, *Tfcp2l1*, *Gbx2*, and *Tbx3*), mirroring the gene expression signature of the post-implantation epiblast (Figure 1M).[32] Next, we performed a cross-species comparison of these transcriptomic data with published mouse PSC lines[10] and mouse E4.5–7.5 epiblast data.[33] The mouse and rat PSC lines correlate nicely based on their origin (e.g., rESCs with mESCs, rEpiSCs with mouse formative stem cells [mFSCs]/EpiSCs). While rEpiSCs are less correlated with mEpiSCs in medium only containing activin-A and bFGF, likely due to the absence of WNT inhibitor, we could not conclude whether rEpiSCs are more similar to either mFSCs or mEpiSCs (Figure 1N). In comparison with *in vivo* cells, rESCs are highly correlated with E4.5–5.5 epiblasts, whereas rEpiSCs show the highest correlation with E6.5 epiblasts (Figure S2H). Collectively, rEpiSCs under our defined conditions exhibit features of the *in vitro* formative or primed PSCs and *in vivo* pluripotent epiblasts in post-implantation embryos.

Resetting the transcriptional regulatory network of rEpiSCs toward naive pluripotency

Since rEpiSCs reflect a different pluripotent state to naive rESCs, we examined key transcriptional regulator(s) capable of reprogramming between these two distinct states. In mice and humans, the overexpression of specific transcription factors (TFs) linked to naive pluripotency resets the transcriptional regulatory network and epigenome of primed PSCs toward naive PSCs. Based on previous mouse studies, we selected six candidate TFs (*Nanog*, *Klf2*, *Klf4*, *Esrrb*, *Tfcp2l1*, and *Tbx3*) highly expressed in naive rESCs but not in rEpiSCs (Figure 1M). All the selected genes are known to reprogram mEpiSCs toward naive ESC-like cells (ESCLCs).[34–39] We cloned each candidate gene into a *PiggyBac* transposon vector containing the doxycycline (Dox)-inducible Tet-On system. To monitor successful reprogramming to rat ESCLCs (rESCLCs), we used rEpiSCs with *Prdm14-H2BVenus* (PV) reporter, which is activated in naive rESCs but not in rEpiSCs (Figures 2B and S2C). After transfection of plasmids and subsequent selection with antibiotics,

CellPress
OPEN ACCESS

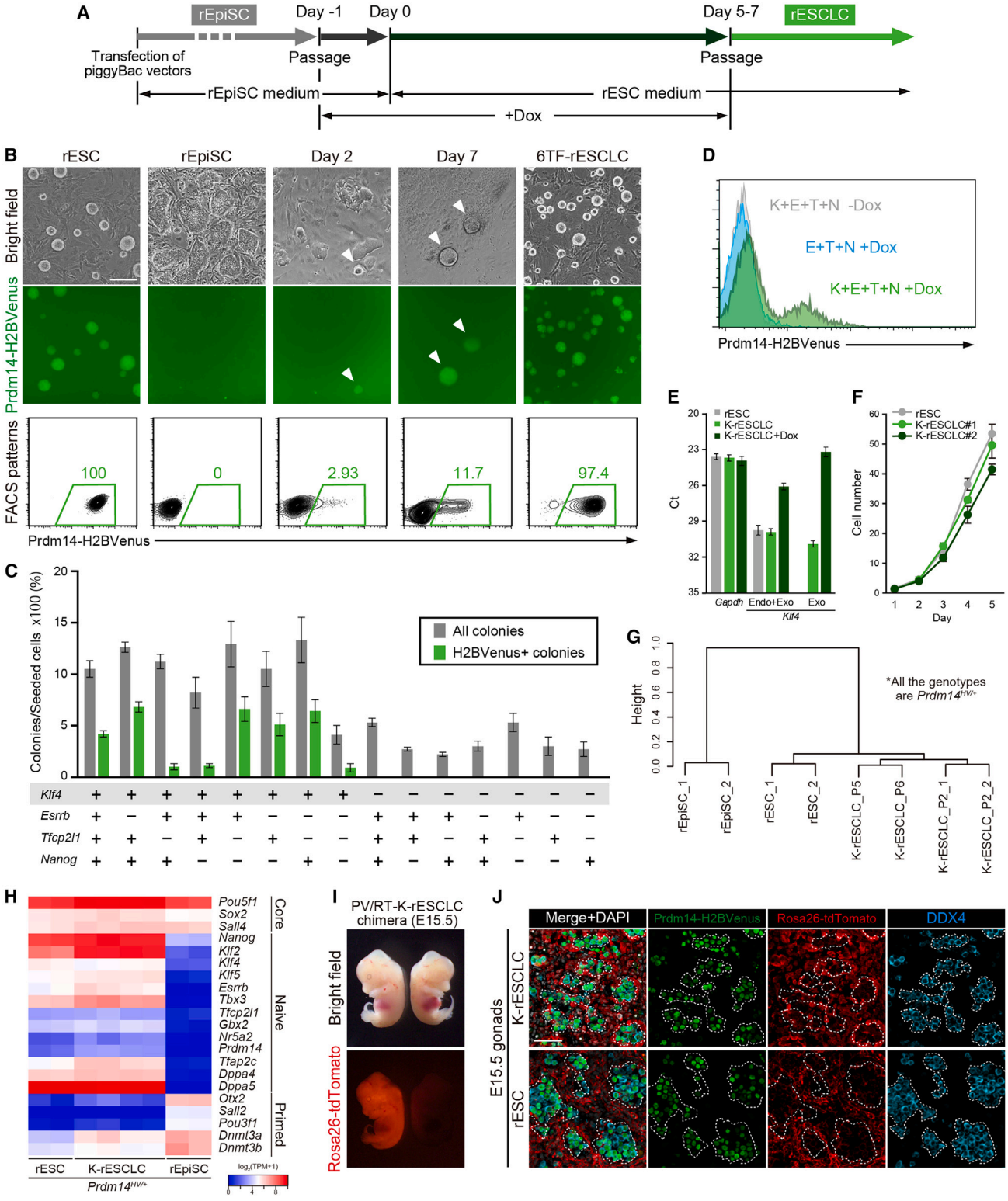

Figure 2. Reprogramming of rEpiSCs toward rESC-like cells by forced expression of *Klf4*

(A) Timeline for rEpiSC reprogramming. The dissociated rEpiSCs were re-plated in rEpiSC medium with doxycycline (Dox) and cultured for 24 h, and then the medium was replaced by rESC medium with Dox. At day 7, PV-positive cells were re-plated in rESC medium without Dox and maintained as rESC-like cells (rESCLCs).

(legend continued on next page)

rEpiSCs with the six TFs (6TF-rEpiSCs) were re-plated on the feeder as single cells in rEpiSC medium with Dox. On the next day, the medium was switched to rESC medium (N2B27 supplemented with 2i/LIF) with Dox (termed day 0) (Figure 2A). On days 2–5, after initiating reprogramming, cells started forming clusters, and some displayed PV fluorescence (arrowheads in Figure 2B and S3A). By day 7, PV-positive colonies exhibited dome-shaped morphology (arrowheads in Figure 2B). After passaging PV-positive colonies by single-cell dissociation using trypsin, cells readily formed typical rESC-like colonies and could be routinely expanded and maintained in rESC medium without Dox (Figure 2B). We found that combined overexpression of the six TFs reprograms primed rEpiSC to naive rESCLCs.

Next, we narrowed down the key candidates of the six TFs crucial for successful reprogramming to naive rESCLCs. We confirmed the expression of the transgenes in rEpiSCs and rESCLCs cultured in the presence or absence of Dox by quantitative reverse transcription PCR (qRT-PCR). In rEpiSCs, the expression of five TFs except for *rTbx3* was significantly upregulated after Dox addition (Figure S3B). However, despite Dox addition, exogenous *rKlf2* and *rTbx3* were not upregulated in rESCLCs (Figure S3B). Therefore, *rKlf2* and *rTbx3* are unlikely candidates for reprogramming among the six TFs. To further narrow down the factors from the remaining four TFs, we tested the reprogramming efficiencies of 15 possible combinations, as indicated in Figure 2C. Notably, for any given combination, the absence of *rKlf4* completely abrogated reprogramming even in the presence of all three TFs (Figures 2C and 2D). Conversely, *rKlf4* alone could reprogram the rEpiSCs to rESCLCs, although at a lower efficiency than in combination with other TFs (Figure 2C), suggesting that the *rKlf4* is sufficient for reprogramming primed EpiSCs to naive rESCLCs in rats. We also found that adding any of the three remaining TFs individually can enhance the reprogramming efficiency by approximately five times in combination with *rKlf4* (Figure 2C). Interestingly, the combination of *rKlf4* with *rEsrrb* showed rapid reprogramming (~2 days) compared with the other TFs paired with *rKlf4* (Figures S3C and S3D), which is consistent with previous reports showing *Esrrb* plays a pioneering role in mEpiSC reprogramming.[40]

We then characterized *rKlf4*-reprogrammed rESCLCs (K-rESCLCs). In K-rESCLCs, exogenous *rKlf4* expression was approximately 200 times lower than in the presence of Dox. Instead, total *rKlf4* expression was comparable to *Klf4* in rESCs (Figure 2E), indicating that a cell-autonomous naive pluripotency transcriptional network was established once the cells were fully reprogrammed. K-rESCLCs proliferated at a similar rate to rESCs (Figure 2F). In the hierarchical clustering of transcriptome data, K-rESCLCs clustered together with rESCs but were distinct from rEpiSCs (Figures 2G and S3E). K-rESCLCs and rESCs expressed naive pluripotency genes but not genes related to the post-implantation epiblast (Figure 2H). To test K-rESCLCs for pluripotency, we performed blastocyst injection. For the donor cells, rEpiSCs with PV and *Rosa26-tdTomato* reporter (PV/RT) were reprogrammed to rESCLCs by overexpression of *rKlf4* (Figure S3F). The PV/RT-K-rESCLCs efficiently contributed to chimera formation at E15.5 (Figure 2I and Table S2). Notably, PV/RT-K-rESCLCs also differentiated into PV and DDX4 double-positive PGCs in the gonads (Figure 2J). We show that *Klf4* is a key transcriptional regulator in reprogramming rEpiSCs to rESCLCs, which are functionally equivalent to naive rESCs.

Germline competency of rat EpiSCs to produce functional PGCLCs

In rodents, the pluripotent epiblast is transiently competent for germline development before the expression of lineage markers and then primed toward somatic lineages. rEpiSCs in the AFI_2XY medium barely expressed early lineage markers such as *Tbxt* and *Foxa2* (Figures 1M and 3A), in contrast to primed mEpiSCs[6,10] but similar to formative pluripotent cells.[10,13] We hypothesized that rEpiSCs cultured in AFI_2XY might reflect the pluripotent state of the pre-gastrulating rat epiblast prior to lineage priming, where rEpiSCs still retain the potential to produce PGCLCs, a defining feature of formative PSCs. To confirm our hypothesis, we tested if the rESC-derived rEpiLCs can maintain germline competency after prolonged culture in the AFI_2XY medium (Figure 3B). To quantify and visualize rPGCLC induction efficiency, we used a *Nanos3-T2A-tdTomato* reporter rESCs (N3T-rESCs).[23] We confirmed that rEpiLCs induced from N3T-rESCs could differentiate into rPGCLCs (hereafter, LC-rPGCLCs) in PGCLC medium (N2B27 supplemented with 5% KSR, 500 ng/mL BMP4, 1000 IU LIF, 100 ng/mL stem cell factor [SCF], and 100 ng/mL epidermal growth factor [EGF]) as previously shown (Figures 3D and 3E).[23] To increase the number of aggregates for the subsequent induction of rPGCLCs, we induced rEpiLCs in micro-well plates (see STAR Methods) and harvested rEpiLC aggregates on feeders in rEpiSC medium (Figure 3C). The cultured rEpiLCs readily formed undifferentiated colonies and constantly proliferated like rEpiSCs (hereafter, LC-rEpiSCs) (Figure 3C). The LC-rEpiSCs were subjected to rPGCLC induction at multiple time points, as indicated in Figures 3D and 3E, by direct formation of spherical aggregates in a low-binding U-bottom plate filled with PGCLC medium. While the induction efficiency varied from experiment to experiment, LC-rEpiSCs could induce

(B) The change of morphology and PV expression during reprogramming. White arrowheads show the dome-shaped colonies displaying PV fluorescence. Scale bar represents 200 μm.
(C) Reprogramming efficiency of possible 15 combinations when using four TFs (*rKlf4*, *rEsrrb*, *rTfcp2l1*, and *rNanog*). Efficiency was calculated as the rate of the dome-shaped/PV-positive colonies per the seeded cell number in 96 wells (mean ± SD of five replicates).
(D) FACS pattern of PV in reprogramming day 7.
(E) qRT-PCR analysis of *Klf4* (K)-rESCLCs when cultured in 2iL medium with or without Dox.
(F) Cell proliferation of rESCLCs independent of exogenous *Klf4*. Data represent mean ± SD of four replicates.
(G) Hierarchical clustering of rESCs, rESCLCs, and rEpiSCs in the same genetic background, PV line.
(H) Heatmap of the pluripotent genes among rESCs, rESCLCs, and rEpiSCs.
(I) Chimera contribution of rESCLCs and rESCs. Images show the fetuses displaying RT fluorescence at E15.5.
(J) Germline contribution in E15.5 chimera fetuses. Scale bar represents 50 μm.

CellPress
OPEN ACCESS

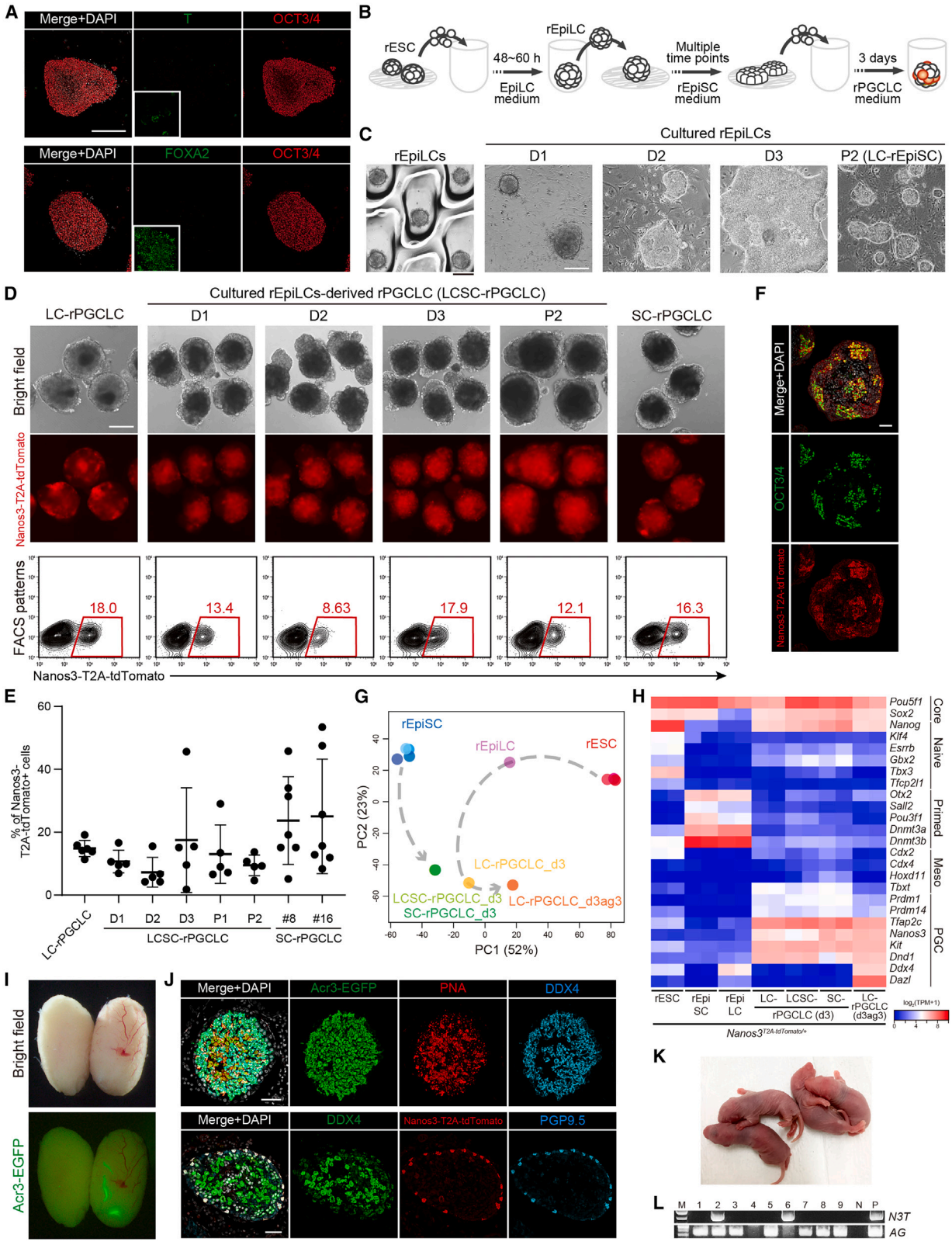

(legend on next page)

N3T-positive rPGCLCs (LCSC-rPGCLCs) (Figures 3D and 3E). Importantly, N3T-positive LCSC-rPGCLCs expressed key germ cell markers as in LC-rPGCLCs (Figure 3H). We conclude that rEpiLCs retained germline competency after prolonged culture in the AFI_2XY medium.

We next tested whether *in vivo* epiblast-derived rEpiSCs also retain germline competency. We freshly isolated epiblasts from E7.5 rat embryos obtained by crossing the N3T reporter rat with *Acrosin-EGFP* (AG) reporter rat,[23] a reporter to visualize spermatogenesis, and derived rEpiSC lines (N3T/AG-rEpiSCs). The N3T/AG-rEpiSCs showed morphology and molecular features typical for rEpiSCs (Figures S4A and S4B). After single-cell dissociation and subsequent formation of spherical aggregates with cytokines, the rEpiSCs produced N3T-positive rPGCLCs 2–3 days after induction (Figures 3D and 3E). We tested five cell lines regardless of sex, and all induced rPGCLCs (Figure S4C). We found that the rEpiSCs retain competency to produce rPGCLCs even after 15 passages in the rEpiSC medium (Figures S4D and S4E). N3T-positive rPGCLCs co-express the pluripotency and germ cell marker, OCT3/4, as judged by IF staining (Figure 3F). Principal component analysis of RNA-seq data revealed that rEpiSC-derived rPGCLCs (hereafter, SC-rPGCLC) are transcriptionally similar to LC-rPGCLC and LCSC-rPGCLCs regardless of their different origins (Figure 3G). We also confirmed that SC-rPGCLCs express all the key early germ cell and pluripotency markers as in LC-rPGCLCs (Figure 3H).

Finally, to test the function of SC-rPGCLCs, we transplanted SC-rPGCLCs into a seminiferous tubule of *Prdm14* KO testis.[32,41] 9–12 weeks after transplantation, some of the seminiferous tubules showed bright AG signals (Figures 3I and Table 1). By IF, we confirmed the presence of N3T-positive spermatogonia at the basal membrane of the tubules, DDX4-positive spermatocyte/spermatids, and PNA-lectin-positive, mature sperm in the EGFP-positive tubules, suggesting SC-rPGCLCs completed spermatogenesis upon transplantation (Figure 3J and S4H). Furthermore, the fluorescence-activated cell sorting (FACS)-sorted SC-rPGCLC-derived round spermatids could contribute to functional embryos upon their injection into unfertilized rat oocytes to develop into healthy offspring inheriting rEpiSC-derived genotype (Figures 3K and 3L). Therefore, rEpiSCs retain germline competency similar to *in vivo* pre-gastrulating epiblast and *in vitro* rEpiLCs and give rise to rPGCLCs that contribute to functional gametes and subsequent offspring.

DISCUSSION

In this study, we report an improved cell culture condition (AFI_2XY) optimal for the expansion and culture of rat EpiSCs. We show that the rEpiSCs transcriptionally correspond to the pre-gastrulation epiblast and are germline competent. Instead of *in vivo* epiblasts, which are difficult to obtain at scale, genetically manipulated, and utilized for biochemical analyses, *in vitro* EpiSCs provide a valuable tool to study the mechanisms underlying germ layer and PGC specification.

We demonstrate that inhibition of the WNT pathway is essential to prevent spontaneous differentiation of rEpiSCs as in mEpiSCs[26–28] but more stringently to block both canonical WNT signaling and WNT secretion. Previously, it has been shown that naive rESCs prefer a lower concentration of GSK3 inhibitor than mESCs, an activator of the canonical WNT pathway, to stabilize the undifferentiated state.[42,43] Thus, rat PSCs might be more sensitive to WNT signaling toward differentiation, regardless of the pluripotent states. Importantly, without WNT inhibition during maintenance, rEpiSCs do not produce rPGCLCs (Figures S4F and S4G), suggesting that active signals in undifferentiated rEpiSCs may also influence the future cell fate decision. Also, we found continuous inhibition of ROCK supports the survival of rEpiSCs. Why continuous ROCK inhibition is required in rEpiSCs remains unknown. Dissociation of primed PSCs induces apoptosis by hyperactivation of the Rho-ROCK-dependent actomyosin pathway.[44] Since the removal of ROCK inhibitor rapidly causes cell death (Figure S1C), the pathway may be consistently activated in rEpiSCs during culture.

Reprogramming among distinct pluripotent states by exogenous TFs gives us insights into their cellular identity and fate conversion. We developed this system using a faithful PV reporter to visualize naive rESCLCs in rats, for the first time. Although overexpression of individual naive pluripotency TFs (*Nanog*, *Klf2*, *Klf4*, *Esrrb*, *Tfcp2l1*, and *Tbx3*) could reprogram primed EpiSCs to naive ESCLCs in mice,[34–39] we found only *Klf4* to reprogram rEpiSCs successfully. The molecular mechanisms for why Klf4 reprograms rEpiSCs, but not the other tested factors, merits further investigation.

In our culture conditions, rEpiSCs retain the competence to produce rPGCLCs, which resemble formative rather than primed PSCs in mice.[45] Notably, this is the first account of PGCLCs induced from self-renewable PSCs with the ability to produce gametes, leading to the birth of viable offspring; this has not

Figure 3. Functional PGC competency of rEpiSCs

(A) IF of rEpiSCs. Scale bar represents 200 μm.

(B) Experimental design for investigating germline competency of rEpiLC-derived rEpiSCs.

(C) Images of the rEpiLC aggregates cultured at multiple time points. rEpiLC-derived rEpiSCs were named LC-rEpiSC. Scale bar represents 200 μm.

(D) Morphology, florescence, and FACS pattern of rEpiLC (LC), LC-rEpiSC (LCSC), and rEpiSC (SC)-derived rPGCLCs. Scale bar represents 200 μm.

(E) Induction efficiency of day 3 (d3) LCs, LCSCs, and SC-rPGCLCs at multiple time points. For SC-rPGCLCs, we used rEpiSCs at passage 6–12.

(F) IF of a cryosection of d3 SC-rPGCLCs. Scale bar represents 50 μm.

(G) PCA of rPSCs and rPGCLCs at day 3 and late-stage rPGCLCs purified from day 3 aggregates of LC-rPGCLC_d3 and female gonadal somatic cells (LC-rPGCLC_d3ag3).[23]

(H) Heatmap of representative gene expression of pluripotency and germ cells.

(I) *Prdm14* KO rat testis at 10 weeks after transplantation of d3 N3T/AG-SC-rPGCLCs.

(J) IF of sections showing testis 10 weeks after transplantation of d3 SC-rPGCLCs. Scale bar represents 50 μm.

(K) Offspring from SC-rPGCLC-derived spermatids generated by round spermatid injection (ROSI).

(L) Genotyping result of offspring to detect transgenes originating from rEpiSCs.

Table 1. Spermatogenesis efficiency after SC-rPGCLC transplantation

rEpiSC lines used for rPGCLC induction (passage number)	Number of testes transplanted	Number of testes with successful transfer	Number of testes with EGFP-positive tubules	Number of EGFP-positive tubules in each testis
#16 (P8)	6	2 of 6 (33%)	1 of 2 (50%)	1
#16 (P8)	3	3 of 3 (100%)	1 of 3 (33%)	3
#16 (P8)	8	5 of 8 (63%)	2 of 5 (40%)	1, >5
#8 (P5)	3	3 of 3 (100%)	1 of 3 (33%)	4

been achieved in any other species, including mice, so far.[5,9–11,46,47] Our rat model system data demonstrate that SC-rPGCLCs are equivalent to authentic LC-rPGCLCs molecularly and functionally. Apart from rodents, rabbits, monkeys, and human PSCs similar to pre- or peri-gastrulating epiblasts can also directly induce PGCLCs.[25,48,49] The definitive proof of function that PGCLCs can be generated from self-renewable epiblast-derived cells in rats expands their potential for future studies. Whether this potential is conserved in other species requires further testing. Interestingly, the culture conditions supporting germline competency differ among rodents and mammals. Therefore, adding insights from the rat model will help elucidate extrinsic signals and intrinsic gene regulatory networks for sustained pluripotency and germline competency across species.

Limitations of the study

In this study, we optimized culture conditions for rEpiSC derivation and maintenance. We find that feeders are necessary to stabilize the cells, and the substrates we tested so far caused partial differentiation and could not replace feeders (Figure S1D). Despite being loosely attached, naive rESCs also require feeders for their maintenance. Thus, it is possible that common mechanism(s)/substrates could support the propagation of rESCs and rEpiSCs in the absence of feeders.

Although the rEpiSCs in our culture conditions are homogenously undifferentiated populations, only 10%–30% of the cells in the aggregates form rPGCLCs upon BMP4 stimuli, like in other mammals.[25,48,49] What factor(s) determine the germline fate decision requires further investigation using the self-renewable stem cell line developed in this study.

In this study, we denote the derived cells as "EpiSCs" reflecting their origin from the epiblast, whereas rEpiSCs molecularly and functionally resemble the formative state. One clear difference between rEpiSC and mFSCs is that rEpiSCs do not form chimeras. The developmental difference of 1–2 days between mouse and rat may affect the competency to form chimeras. While the continuum and progression of pluripotency states during early development appear broadly conserved among mammals, the timescales required for the transitions and optimal conditions to capture the formative state *in vitro*, i.e., responsiveness to external signals, may vary depending on the species. Hence, cross-species analyses and identifying key TFs or gene regulatory networks will elucidate nuances of pluripotent states across evolution.

STAR★METHODS

Detailed methods are provided in the online version of this paper and include the following:

SUPPLEMENTAL INFORMATION

Supplemental information can be found online at https://doi.org/10.1016/j.crmeth.2023.100542.

ACKNOWLEDGMENTS

We thank members of the Kobayashi lab and Hirabayashi lab, particularly Keiko Yamauchi, Fumika Yoshida, and Hijiri Saito for technical assistance and Minako Ohnishi for secretarial support. We also thank Dr. Roopsha Sengupta for editing and providing critical input to the manuscript. Flow cytometry was performed in the IMSUT FACS Core laboratory. This work was supported by KAKENHI from the JSPS grants 18H02367 to M.H. and T.K., 18H05548 and 20H03167 to T.K., 18H05544 to T.K. and K.K., 19K23711 to M.O., 21H02382 to H.K., 21J21849 to K.I., 21J21849, AMED JP18bm0704022, and JP22bm1123008 to T.K., Cooperative Study Program (21-147) of NIPS to T.K., and grants from the Sumitomo Foundation (210348) to T.K., Kato Memorial Bioscience Foundation to T.K., and Daiichi Sankyo Foundation of Life Science to T.K.

AUTHORS CONTRIBUTIONS

Conceptualization: K.I. and T.K.; methodology: K.I., M.O., H.K., C.A.P., M.S., M.H., and T.K.; formal analysis: K.I.; investigation: K.I. and T.K.; visualization:

K.I.; writing: K.I. and T.K.; supervision: T.Y., S.H., K.K., and T.K.; funding acquisition: K.I., M.O., M.H., K.K., and T.K.

DECLARATION OF INTERESTS

The authors declare no competing interests.

INCLUSION AND DIVERSITY

We support inclusive, diverse, and equitable conduct of research.

Received: January 11, 2023
Revised: May 10, 2023
Accepted: July 3, 2023
Published: July 27, 2023

REFERENCES

1. Kinoshita, M., and Smith, A. (2018). Pluripotency Deconstructed. Dev. Growth Differ. *60*, 44–52. https://doi.org/10.1111/dgd.12419.
2. Boroviak, T., Loos, R., Bertone, P., Smith, A., and Nichols, J. (2014). The ability of inner-cell-mass cells to self-renew as embryonic stem cells is acquired following epiblast specification. Nat. Cell Biol. *16*, 516–528. https://doi.org/10.1038/ncb2965.
3. Bradley, A., Evans, M., Kaufman, M.H., and Robertson, E. (1984). Formation of germ-line chimaeras from embryo-derived teratocarcinoma cell lines. Nature *309*, 255–256. https://doi.org/10.1038/309255a0.
4. Brons, I.G.M., Smithers, L.E., Trotter, M.W.B., Rugg-Gunn, P., Sun, B., Chuva de Sousa Lopes, S.M., Howlett, S.K., Clarkson, A., Ahrlund-Richter, L., Pedersen, R.A., and Vallier, L. (2007). Derivation of pluripotent epiblast stem cells from mammalian embryos. Nature *448*, 191–195. https://doi.org/10.1038/nature05950.
5. Tesar, P.J., Chenoweth, J.G., Brook, F.A., Davies, T.J., Evans, E.P., Mack, D.L., Gardner, R.L., and McKay, R.D.G. (2007). New cell lines from mouse epiblast share defining features with human embryonic stem cells. Nature *448*, 196–199. https://doi.org/10.1038/nature05972.
6. Kojima, Y., Kaufman-Francis, K., Studdert, J.B., Steiner, K.A., Power, M.D., Loebel, D.A.F., Jones, V., Hor, A., de Alencastro, G., Logan, G.J., et al. (2014). The transcriptional and functional properties of mouse epiblast stem cells resemble the anterior primitive streak. Cell Stem Cell *14*, 107–120. https://doi.org/10.1016/j.stem.2013.09.014.
7. Nichols, J., and Smith, A. (2009). Naive and primed pluripotent states. Cell Stem Cell *4*, 487–492. https://doi.org/10.1016/j.stem.2009.05.015.
8. Mascetti, V.L., and Pedersen, R.A. (2016). Contributions of Mammalian Chimeras to Pluripotent Stem Cell Research. Cell Stem Cell *19*, 163–175. https://doi.org/10.1016/j.stem.2016.07.018.
9. Wang, X., Xiang, Y., Yu, Y., Wang, R., Zhang, Y., Xu, Q., Sun, H., Zhao, Z.A., Jiang, X., Wang, X., et al. (2021). Formative pluripotent stem cells show features of epiblast cells poised for gastrulation. Cell Res. *31*, 526–541. https://doi.org/10.1038/s41422-021-00477-x.
10. Kinoshita, M., Barber, M., Mansfield, W., Cui, Y., Spindlow, D., Stirparo, G.G., Dietmann, S., Nichols, J., and Smith, A. (2021). Capture of mouse and human stem cells with features of formative pluripotency. Cell Stem Cell *28*, 453–471.e8. https://doi.org/10.1016/j.stem.2020.11.005.
11. Yu, L., Wei, Y., Sun, H.X., Mahdi, A.K., Pinzon Arteaga, C.A., Sakurai, M., Schmitz, D.A., Zheng, C., Ballard, E.D., Li, J., et al. (2021). Derivation of intermediate pluripotent stem cells amenable to primordial germ cell specification. Cell Stem Cell *28*, 550–567.e12. https://doi.org/10.1016/j.stem.2020.11.003.
12. Ohinata, Y., Ohta, H., Shigeta, M., Yamanaka, K., Wakayama, T., and Saitou, M. (2009). A signaling principle for the specification of the germ cell lineage in mice. Cell *137*, 571–584. https://doi.org/10.1016/j.cell.2009.03.014.
13. Hayashi, K., Ohta, H., Kurimoto, K., Aramaki, S., and Saitou, M. (2011). Reconstitution of the mouse germ cell specification pathway in culture by pluripotent stem cells. Cell *146*, 519–532. https://doi.org/10.1016/j.cell.2011.06.052.
14. Kalkan, T., Olova, N., Roode, M., Mulas, C., Lee, H.J., Nett, I., Marks, H., Walker, R., Stunnenberg, H.G., Lilley, K.S., et al. (2017). Tracking the embryonic stem cell transition from ground state pluripotency. Development *144*, 1221–1234. https://doi.org/10.1242/dev.142711.
15. Weinberger, L., Ayyash, M., Novershtern, N., and Hanna, J.H. (2016). Dynamic stem cell states: naive to primed pluripotency in rodents and humans. Nat. Rev. Mol. Cell Biol. *17*, 155–169. https://doi.org/10.1038/nrm.2015.28.
16. De Los Angeles, A., Ferrari, F., Xi, R., Fujiwara, Y., Benvenisty, N., Deng, H., Hochedlinger, K., Jaenisch, R., Lee, S., Leitch, H.G., et al. (2015). Hallmarks of pluripotency. Nature *525*, 469–478. https://doi.org/10.1038/nature15515.
17. Buehr, M., Meek, S., Blair, K., Yang, J., Ure, J., Silva, J., McLay, R., Hall, J., Ying, Q.L., and Smith, A. (2008). Capture of authentic embryonic stem cells from rat blastocysts. Cell *135*, 1287–1298. https://doi.org/10.1016/j.cell.2008.12.007.
18. Li, P., Tong, C., Mehrian-Shai, R., Jia, L., Wu, N., Yan, Y., Maxson, R.E., Schulze, E.N., Song, H., Hsieh, C.L., et al. (2008). Germline competent embryonic stem cells derived from rat blastocysts. Cell *135*, 1299–1310. https://doi.org/10.1016/j.cell.2008.12.006.
19. Ying, Q.L., Wray, J., Nichols, J., Batlle-Morera, L., Doble, B., Woodgett, J., Cohen, P., and Smith, A. (2008). The ground state of embryonic stem cell self-renewal. Nature *453*, 519–523. https://doi.org/10.1038/nature06968.
20. Takashima, Y., Guo, G., Loos, R., Nichols, J., Ficz, G., Krueger, F., Oxley, D., Santos, F., Clarke, J., Mansfield, W., et al. (2014). Resetting transcription factor control circuitry toward ground-state pluripotency in human. Cell *158*, 1254–1269. https://doi.org/10.1016/j.cell.2014.08.029.
21. Theunissen, T.W., Powell, B.E., Wang, H., Mitalipova, M., Faddah, D.A., Reddy, J., Fan, Z.P., Maetzel, D., Ganz, K., Shi, L., et al. (2014). Systematic identification of culture conditions for induction and maintenance of naive human pluripotency. Cell Stem Cell *15*, 471–487. https://doi.org/10.1016/j.stem.2014.07.002.
22. Guo, G., von Meyenn, F., Santos, F., Chen, Y., Reik, W., Bertone, P., Smith, A., and Nichols, J. (2016). Naive Pluripotent Stem Cells Derived Directly from Isolated Cells of the Human Inner Cell Mass. Stem Cell Rep. *6*, 437–446. https://doi.org/10.1016/j.stemcr.2016.02.005.
23. Oikawa, M., Kobayashi, H., Sanbo, M., Mizuno, N., Iwatsuki, K., Takashima, T., Yamauchi, K., Yoshida, F., Yamamoto, T., Shinohara, T., et al. (2022). Functional primordial germ cell-like cells from pluripotent stem cells in rats. Science *376*, 176–179. https://doi.org/10.1126/science.abl4412.
24. Ying, Q.L., Stavridis, M., Griffiths, D., Li, M., and Smith, A. (2003). Conversion of embryonic stem cells into neuroectodermal precursors in adherent monoculture. Nat. Biotechnol. *21*, 183–186. https://doi.org/10.1038/nbt780.
25. Kobayashi, T., Castillo-Venzor, A., Penfold, C.A., Morgan, M., Mizuno, N., Tang, W.W.C., Osada, Y., Hirao, M., Yoshida, F., Sato, H., et al. (2021). Tracing the emergence of primordial germ cells from bilaminar disc rabbit embryos and pluripotent stem cells. Cell Rep. *37*, 109812. https://doi.org/10.1016/j.celrep.2021.109812.
26. Sugimoto, M., Kondo, M., Koga, Y., Shiura, H., Ikeda, R., Hirose, M., Ogura, A., Murakami, A., Yoshiki, A., Chuva de Sousa Lopes, S.M., and Abe, K. (2015). A simple and robust method for establishing homogeneous mouse epiblast stem cell lines by wnt inhibition. Stem Cell Rep. *4*, 744–757. https://doi.org/10.1016/j.stemcr.2015.02.014.
27. Wu, J., Okamura, D., Li, M., Suzuki, K., Luo, C., Ma, L., He, Y., Li, Z., Benner, C., Tamura, I., et al. (2015). An alternative pluripotent state confers interspecies chimaeric competency. Nature *521*, 316–321. https://doi.org/10.1038/nature14413.
28. Sumi, T., Oki, S., Kitajima, K., and Meno, C. (2013). Epiblast ground state is controlled by canonical Wnt/beta-catenin signaling in the

postimplantation mouse embryo and epiblast stem cells. PLoS One *8*, e63378. https://doi.org/10.1371/journal.pone.0063378.

29. Greber, B., Coulon, P., Zhang, M., Moritz, S., Frank, S., Müller-Molina, A.J., Araúzo-Bravo, M.J., Han, D.W., Pape, H.C., and Schöler, H.R. (2011). FGF signalling inhibits neural induction in human embryonic stem cells. EMBO J. *30*, 4874–4884. https://doi.org/10.1038/emboj.2011.407.
30. Watanabe, K., Ueno, M., Kamiya, D., Nishiyama, A., Matsumura, M., Wataya, T., Takahashi, J.B., Nishikawa, S.i., Nishikawa, S., Muguruma, K., and Sasai, Y. (2007). A ROCK inhibitor permits survival of dissociated human embryonic stem cells. Nat. Biotechnol. *25*, 681–686. https://doi.org/10.1038/nbt1310.
31. Kinoshita, M., Kobayashi, T., Planells, B., Klisch, D., Spindlow, D., Masaki, H., Bornelov, S., Stirparo, G.G., Matsunari, H., Uchikura, A., et al. (2021). Pluripotent stem cells related to embryonic disc exhibit common self-renewal requirements in diverse livestock species. Development *148*. https://doi.org/10.1242/dev.199901.
32. Kobayashi, T., Kobayashi, H., Goto, T., Takashima, T., Oikawa, M., Ikeda, H., Terada, R., Yoshida, F., Sanbo, M., Nakauchi, H., et al. (2020). Germline development in rat revealed by visualization and deletion of Prdm14. Development *147*. https://doi.org/10.1242/dev.183798.
33. Argelaguet, R., Clark, S.J., Mohammed, H., Stapel, L.C., Krueger, C., Kapourani, C.A., Imaz-Rosshandler, I., Lohoff, T., Xiang, Y., Hanna, C.W., et al. (2019). Multi-omics profiling of mouse gastrulation at single-cell resolution. Nature *576*, 487–491. https://doi.org/10.1038/s41586-019-1825-8.
34. Guo, G., Yang, J., Nichols, J., Hall, J.S., Eyres, I., Mansfield, W., and Smith, A. (2009). Klf4 reverts developmentally programmed restriction of ground state pluripotency. Development *136*, 1063–1069. https://doi.org/10.1242/dev.030957.
35. Silva, J., Nichols, J., Theunissen, T.W., Guo, G., van Oosten, A.L., Barrandon, O., Wray, J., Yamanaka, S., Chambers, I., and Smith, A. (2009). Nanog is the gateway to the pluripotent ground state. Cell *138*, 722–737. https://doi.org/10.1016/j.cell.2009.07.039.
36. Dunn, S.J., Li, M.A., Carbognin, E., Smith, A., and Martello, G. (2019). A common molecular logic determines embryonic stem cell self-renewal and reprogramming. EMBO J. *38*, e100003. https://doi.org/10.15252/embj.2018100003.
37. Hall, J., Guo, G., Wray, J., Eyres, I., Nichols, J., Grotewold, L., Morfopoulou, S., Humphreys, P., Mansfield, W., Walker, R., et al. (2009). Oct4 and LIF/Stat3 additively induce Krüppel factors to sustain embryonic stem cell self-renewal. Cell Stem Cell *5*, 597–609. https://doi.org/10.1016/j.stem.2009.11.003.
38. Ye, S., Li, P., Tong, C., and Ying, Q.L. (2013). Embryonic stem cell self-renewal pathways converge on the transcription factor Tfcp2l1. EMBO J. *32*, 2548–2560. https://doi.org/10.1038/emboj.2013.175.
39. Festuccia, N., Osorno, R., Halbritter, F., Karwacki-Neisius, V., Navarro, P., Colby, D., Wong, F., Yates, A., Tomlinson, S.R., and Chambers, I. (2012). Esrrb is a direct Nanog target gene that can substitute for Nanog function in pluripotent cells. Cell Stem Cell *11*, 477–490. https://doi.org/10.1016/j.stem.2012.08.002.
40. Adachi, K., Kopp, W., Wu, G., Heising, S., Greber, B., Stehling, M., Araúzo-Bravo, M.J., Boerno, S.T., Timmermann, B., Vingron, M., and Schöler, H.R. (2018). Esrrb Unlocks Silenced Enhancers for Reprogramming to Naive Pluripotency. Cell Stem Cell *23*, 266–275.e6. https://doi.org/10.1016/j.stem.2018.05.020.
41. Kobayashi, T., Goto, T., Oikawa, M., Sanbo, M., Yoshida, F., Terada, R., Niizeki, N., Kajitani, N., Kazuki, K., Kazuki, Y., et al. (2021). Blastocyst complementation using Prdm14-deficient rats enables efficient germline transmission and generation of functional mouse spermatids in rats. Nat. Commun. *12*, 1328. https://doi.org/10.1038/s41467-021-21557-x.
42. Chen, Y., Blair, K., and Smith, A. (2013). Robust self-renewal of rat embryonic stem cells requires fine-tuning of glycogen synthase kinase-3 inhibition. Stem Cell Rep. *1*, 209–217. https://doi.org/10.1016/j.stemcr.2013.07.003.
43. Meek, S., Wei, J., Sutherland, L., Nilges, B., Buehr, M., Tomlinson, S.R., Thomson, A.J., and Burdon, T. (2013). Tuning of beta-catenin activity is required to stabilize self-renewal of rat embryonic stem cells. Stem Cell. *31*, 2104–2115. https://doi.org/10.1002/stem.1466.
44. Ohgushi, M., Matsumura, M., Eiraku, M., Murakami, K., Aramaki, T., Nishiyama, A., Muguruma, K., Nakano, T., Suga, H., Ueno, M., et al. (2010). Molecular pathway and cell state responsible for dissociation-induced apoptosis in human pluripotent stem cells. Cell Stem Cell *7*, 225–239. https://doi.org/10.1016/j.stem.2010.06.018.
45. Endoh, M., and Niwa, H. (2022). Stepwise pluripotency transitions in mouse stem cells. EMBO Rep. *23*, e55010. https://doi.org/10.15252/embr.202255010.
46. Kagiwada, S., Aramaki, S., Wu, G., Shin, B., Kutejova, E., Obridge, D., Adachi, K., Wrana, J.L., Hübner, K., and Schöler, H.R. (2021). YAP establishes epiblast responsiveness to inductive signals for germ cell fate. Development *148*. https://doi.org/10.1242/dev.199732.
47. Hayashi, K., and Surani, M.A. (2009). Self-renewing epiblast stem cells exhibit continual delineation of germ cells with epigenetic reprogramming in vitro. Development *136*, 3549–3556. https://doi.org/10.1242/dev.037747.
48. Irie, N., Weinberger, L., Tang, W.W.C., Kobayashi, T., Viukov, S., Manor, Y.S., Dietmann, S., Hanna, J.H., and Surani, M.A. (2015). SOX17 is a critical specifier of human primordial germ cell fate. Cell *160*, 253–268. https://doi.org/10.1016/j.cell.2014.12.013.
49. Sakai, Y., Nakamura, T., Okamoto, I., Gyobu-Motani, S., Ohta, H., Yabuta, Y., Tsukiyama, T., Iwatani, C., Tsuchiya, H., Ema, M., et al. (2020). Induction of the germ cell fate from pluripotent stem cells in cynomolgus monkeys. Biol. Reprod. *102*, 620–638. https://doi.org/10.1093/biolre/ioz205.
50. Kobayashi, T., Zhang, H., Tang, W.W.C., Irie, N., Withey, S., Klisch, D., Sybirna, A., Dietmann, S., Contreras, D.A., Webb, R., et al. (2017). Principles of early human development and germ cell program from conserved model systems. Nature *546*, 416–420. https://doi.org/10.1038/nature22812.
51. Dobin, A., Davis, C.A., Schlesinger, F., Drenkow, J., Zaleski, C., Jha, S., Batut, P., Chaisson, M., and Gingeras, T.R. (2013). STAR: ultrafast universal RNA-seq aligner. Bioinformatics *29*, 15–21. https://doi.org/10.1093/bioinformatics/bts635.
52. Stuart, T., Butler, A., Hoffman, P., Hafemeister, C., Papalexi, E., Mauck, W.M., 3rd, Hao, Y., Stoeckius, M., Smibert, P., and Satija, R. (2019). Comprehensive Integration of Single-Cell Data. Cell *177*, 1888–1902.e21. https://doi.org/10.1016/j.cell.2019.05.031.
53. Miyawaki, S., Okada, Y., Okano, H., and Miura, K. (2017). Teratoma Formation Assay for Assessing Pluripotency and Tumorigenicity of Pluripotent Stem Cells. Bio. Protoc. *7*, e2518. https://doi.org/10.21769/BioProtoc.2518.
54. Miyoshi, K., Abeydeera, L.R., Okuda, K., and Niwa, K. (1995). Effects of osmolarity and amino acids in a chemically defined medium on development of rat one-cell embryos. J. Reprod. Fertil. *103*, 27–32. https://doi.org/10.1530/jrf.0.1030027.
55. Hirabayashi, M., Kato, M., and Hochi, S. (2008). Factors Affecting Full-Term Development of Rat Oocytes Microinjected with Fresh or Cryopreserved Round Spermatids. Exp. Anim. *57*, 401–405. https://doi.org/10.1538/expanim.57.401.
56. Grabole, N., Tischler, J., Hackett, J.A., Kim, S., Tang, F., Leitch, H.G., Magnúsdóttir, E., and Surani, M.A. (2013). Prdm14 promotes germline fate and naive pluripotency by repressing FGF signalling and DNA methylation. EMBO Rep. *14*, 629–637. https://doi.org/10.1038/embor.2013.67.

STAR★METHODS

KEY RESOURCES TABLE

REAGENT or RESOURCE	SOURCE	IDENTIFIER
Antibodies		
OCT3/4	Santa Cruz Biotechnology	Cat# sc-5279; RRID: AB_628051
SOX2	Abcam	Cat# ab97959; RRID: AB_2341193
OTX2	R and D Systems	Cat# AF1979; RRID: AB_2157172
SOX17	R and D Systems	Cat# AF1924; RRID: AB_355060
BRACHYURY	R and D Systems	Cat# AF2085; RRID: AB_2200235
PAX6	Abcam	Cat# ab195045; RRID: AB_2750924
GFP	Abcam	Cat# ab13970; RRID: AB_300798
dsRed	Takara Bio	Cat# 632496; RRID: AB_10013483
DDX4/MVH	Abcam	Cat# ab27591; RRID: AB_11139638
FOXA2/HNF3β	Cell Signaling	Cat# 8186S; RRID: N/A
PNA	Vector Laboratories	Cat# RL-1072; RRID: AB_2336642
mCherry	EnCor Biotechnology	Cat# CPCA-mCherry; RRID: AB_2572308
PGP9.5	Abcam	Cat# ab108986; RRID: AB_10891773
SOX9	Abcam	Cat# ab185966; RRID: AB_2728660
SSEA1	Thermo Fisher Scientific	Cat# 50-8813-42; RRID: AB_11219681
CD81	BioLegend	Cat# 104905; RRID: AB_2076267
Bacterial and virus strains		
DynaCompetent Cells JetGiga DH5α	Biodynamics Laboratory	Cat# DS230
Chemicals, peptides, and recombinant proteins		
Recombinant Human/Murine/Rat Activin A	Peprotech	Cat# 120-14
Recombinant Human FGF-basic	Peprotech	Cat# 100-18B
IWP2	Tocris Bioscience	Cat# 3533; CAS: 686770-61-6
XAV939	Abcam	Cat# ab120897; CAS: 284028-89-3
Y-27632 dihydrochloride	Tocris Bioscience	Cat# 1254; CAS: 129830-38-2
CHIR 99021	Axon Medchem	Cat# 1386; CAS: 252917-06-9
PD 0325901	Axon Medchem	Cat# 1408; CAS: 391210-10-9
Rat LIF (Rat ESGRO)	Millipore	Cat# ESG2207
LDN-193189 dihydrochloride	Tocris Bioscience	Cat# 6053; CAS: 1435934-00-1
Recombinant Human BMP4	Peprotech	Cat# 120-05ET
Recombinant Human EGF	R and D Systems	Cat# 236-EG
Recombinant Mouse SCF	R and D Systems	Cat# 455-MC
Critical commercial assays		
SMART-Seq HT PLUS Kit	Takara Bio	Cat# R400749
NextSeq 500/550 High Output Kit v2.5	Illumina	Cat# 20024907
Deposited data		
RNA-seq data	This paper	GEO; GSE220805
RNA-seq data	Kinoshita et al.[10]	GEO; GSE131556
RNA-seq data	Argelaguet et al.[33]	GEO; GSE121650
Experimental models: Cell lines		
PV rESC line	Kobayashi et al.[32,41]	N/A
PV rEpiSC line	This paper	N/A
N3T rES line	Oikawa et al.[23]	N/A
N3T/AG rEpiSC line	This paper	N/A

(*Continued on next page*)

Continued

REAGENT or RESOURCE	SOURCE	IDENTIFIER
WT rEpiSC line	This paper	N/A
Experimental models: Organisms/strains		
Rat: Crlj:WI	Charles River Laboratories	RGD ID: 2312504
Mouse: NOD/SCID (NOD.CB17-*Prkdc*^{scid}/J)	Charles River Laboratories	JAX® Mice stock number: 001303
Oligonucleotides		
Primers for qRT-PCR, see Table S3	This paper	N/A
Recombinant DNA		
pPBTRE3G-SV40pA	Kobayashi et al.[50]	N/A
Software and algorithms		
FlowJo 10.7.1	BD	https://www.flowjo.com/
GraphPad Prism v8.4.3	Graphpad	https://www.graphpad.com
Adobe Photoshop v23.5.3	Adobe	https://www.adobe.com/
R v3.6.1	The R Foundation	https://www.r-project.org
RaNA-seq	RaNA-seq	https://ranaseq.eu/index.php
NextSeq 500/550 RTA software v2.11.3	Illumina	https://jp.support.illumina.com/sequencing/sequencing_instruments/nextseq-500/downloads.html
TrimGalore!	Babraham Bioinformatics	https://www.bioinformatics.babraham.ac.uk/projects/trim_galore/
STAR v2.5.4b	Dobin et al.[51]	https://github.com/alexdobin/STAR
Seurat v3.1.2	Stuart et al.[52]	https://satijalab.org/seurat/
Custom code for cross-species comparison	This paper	https://doi.org/10.5281/zenodo.8054470

RESOURCE AVAILABILITY

Lead contact

Further information and requests for resources and reagents should be directed to the lead contact, Toshihiro Kobayashi (tkoba@g.ecc.u-tokyo.ac.jp).

Materials availability

Unique reagents generated in this study are available from the lead contact with a Materials Transfer Agreement.

Data and code availability

- This paper analyzes existing, publicly available data. These accession numbers for the datasets are listed in the key resources table. RNA-seq data had been deposited in the Gene Expression Omnibus (GEO) under accession number GSE220805.
- All original code has been deposited at GitHub and is publicly available as of the date of publication. DOI is listed in the key resources table.
- Any additional information required to reanalyze the data reported in this paper is available from the lead contact upon request.

EXPERIMENTAL MODEL AND STUDY PARTICIPANT DETAILS

Chemicals and animals

Unless otherwise indicated, chemicals and kits used in this study were purchased from Thermo Fisher Scientific Inc. (Waltman, MA). Six weeks old to 12 month old rats and NOD/SCID male mice (4–6 weeks old) were used in this study. Crlj:WI (RGD ID: 2312504) rats and NOD/SCID mice were purchased from Charles River Laboratories Japan, Inc. (Kanagawa, Japan). All experiments were performed in accordance with the animal care and use committee guidelines of the National Institutes for Natural Sciences and University of Tokyo.

Derivation and maintenance of rat pluripotent stem cells

Two male naive rESC lines (PV and N3T) were derived in previous our reports, respectively.[23,32] rESCs were maintained on mitomycin-C-treated MEFs in rESC medium; N2B27 medium supplemented with 1 μM PD0325901 (Axon, Groeningen, The Netherlands), 3 μM CHIR99021 (Axon), and 1000 U/ml of rat LIF (Millipore, Bedford, MA). For passaging, confluent rESC colonies were dissociated by 0.25% Trypsin-EDTA and re-plated to a well of 12-well plates (IWAKI, Shizuoka, Japan) containing 1 mL of rESC medium per well. The rESCs were routinely passaged every 3 days.

For the derivation of rEpiSCs, E7.5–8.5 rat epiblasts were isolated as described previously.[32] Briefly, the ectoplacental cone and extra-embryonic ectoderm were mechanically dissected out and used for genotyping. The embryonic visceral endoderm surrounding the epiblast was removed by enzyme solution containing 1.0 mg/mL collagenase type IV (Worthington Biochemical Corporation, Lakewood, NJ), 1.0 mg/mL dispase (FUJIFILM Wako, Osaka, Japan), and 0.3 mg/mL hyaluronidase (Sigma-Aldrich, St. Lois, MO) for 5 min at 37°C followed by repeated pipetting with a glass capillary. The isolated epiblasts were individually explanted on MEF in rEpiSC medium; N2B27 medium supplemented with 5% KSR, 20 ng/mL Activin-A (Peprotech, Cranbury, NJ), 12 ng/mL bFGF (Peprotech), two WNT inhibitors (2 μM IWP2 [Tocris Bioscience, Bristol, UK] and 5 μM XAV-939 [Abcam, Cambridge, UK], and 5 μM Y-27632 (Tocris Bioscience). After 5 days, the expanded epiblast outgrowth was mechanically dissociated using a glass capillary. From the second passage, rEpiSC colonies were dissociated by Accutase (Innovative Cell Technologies, San Diego, CA) and re-plated to a well of MEF coated 12-well plates containing 1 mL of rEpiSC medium per well. The rEpiSCs were routinely passaged every 3–4 days.

METHOD DETAILS

In vitro differentiation of rEpiSCs into 3 germ layers

To differentiate rEpiSCs into 3 germ layers, embryoid bodies (EB) were obtained from rEpiSCs by seeding 2x10e4 rEpiSCs/well in EZSPHERESP micro-well 96 well plate (IWAKI) for 24 h. Subsequently, the EBs were replated on fibronectin-coated dish and cultured in each induction medium. As a basal medium for differentiation, aRB27 medium composed from advanced RPMI1640 medium supplemented with 1% B27 supplement, 0.1 mM NEAA, antibiotics (100 U/ml Penicillin and 100 μg/mL Streptomycin), and 2 mM L-Glutamine was used. To induce ectoderm lineage, EBs were simply cultured in aRB27 medium for 2 days. To induce mesodermal lineage, EBs were cultured in aRB27 medium supplemented with 100 ng/mL Activin-A, 3 μM CHIR99021, and 10 μM Y-27632 for 2 days. To induce endodermal lineages, EBs were cultured in the medium for mesodermal induction for 24 h, then transferred aRB27 medium supplemented with 100 ng/mL Activin-A, 0.5 μM BMPi (LDN193189; Tocris Bioscience) for 24 h.

Teratoma formation

Teratoma formation from rEpiSCs was conducted as described previously.[53] Briefly, approximately 1x10e5 rEpiSCs were transplanted into testes of NOD/SCID mice. Two-three months later, the teratomas were dissected and analyzed by hematoxylin and eosin staining.

Blastocyst injection to generate chimeras

For blastocyst injection, rat blastocysts were collected in mR1ECM medium[54] from the oviduct and uterus of rats at 4.5 days post-coitum (dpc). For micro-manipulation, rESCs, rEpiSCs and rESCLCs were dissociated and suspended in their culture medium. A piezo-driven micro-manipulator (Prime Tech, Ibaraki, Japan) was used to drill into the zona pellucida and trophectoderm under the microscope, and 8–10 cells were introduced into blastocyst cavities near the ICM. After injection, the blastocysts were transferred into the uterus of pseudopregnant recipient Crlj:WI rats (3.5 dpc). To detect chimerism, rat fetuses were collected at 15.5 dpc (12 days after embryo transfer) and observed under the fluorescent microscope.

Induction of rEpiLCs and rPGCLCs

rEpiLCs and rPGCLCs inductions were performed according to our recent report.[23] Briefly, trypsinized rESCs were seeded in 96-well Nunclon Sphera-Treated U-shaped microplate containing 100 μL of rEpiLC medium (N2B27 medium supplemented with 1% KSR, 20 ng/mL Activin-A, and 12 ng/mL bFGF) at 4x10e3 cells per well. After culture for 48–60 h, rEpiLC-aggregates were transferred into a well of 96-well Nunclon Sphera-Treated U-shaped microplate containing 100 μL of rPGCLC medium (N2B27 medium supplemented with 500 ng/mL BMP4 [Peprotech], 1000 U/ml rLIF, 100 ng/mL SCF [R&D Systems, Minneapolis, MN], and 50 ng/mL EGF [R&D Systems)]. After 3 days, rEpiLC-derived rPGCLCs (LC-rPGCLCs) were analyzed by FACS and IF. To directly induce rPGCLCs from rEpiSCs, trypsinized rEpiSCs including feeders, were seeded in 96-well Nunclon Sphera-Treated U-shaped microplate containing 100 μL of rPGCLC medium at 0.5–1.5x10e4 cells per well. After 3 days, rEpiSC-derived rPGCLCs (SC-rPGCLCs) were analyzed.

Transplantation of the rPGCLCs into seminiferous tubules

Transplantation of SC-rPGCLCs was performed according to our recent report.[23] Briefly, FACS-sorted N3T(+) d3 SC-rPGCLCs were collected and suspended into rPGCLC medium at the concentration of $1x10^4$ cells per 1.5 μL. 0.5 μL of Trypan blue was added (total ~2 μL) to the cell suspensions to confirm the successful injection into the efferent duct, visually. For the recipient, genotyped day 6–9 *Prdm14*$^{H2BVenus/mut}$ (KO) neonatal rats were anesthetized with Isoflurane. A glass capillary filled with 2 μL of rPGCLC suspensions was carefully punctured into the efferent duct of the testis and the cell suspensions were injected using FemtoJet injection system

(Eppendorf, Hamburg, Germany). After injection, neonatal rats that underwent surgery were kept on the 37°C warming plate for at least 30 min and returned to the mother rats. At 10 weeks after transplantation, we confirmed that spermatogenesis originated from the transplanted rPGCLCs by fluorescent microscopy. AG(+) seminiferous tubules were analyzed by immunostaining or were used for round spermatid injection (ROSI).[55]

Reprogramming of rEpiSCs

For the reprogramming of rEpiSCs, the six candidate genes (*rKlf2*, *rKlf4*, *rEsrrb*, *rTbx3*, *rTfcp2l1*, and *rNanog*) were cloned individually into a *PiggyBac* transposon vector containing Doxycycline (Dox)-inducible Tet-On system. The plasmids were transfected into rEpiSCs by reverse transfection protocol using lipofectamine 2000.[50] Transfected rEpiSCs were harvested on neomycin-resistant feeder (Kitayama labes, Nagano, Japan, or in house). Two days after transfection, 400 μg/mL G418 (Sigma-Aldrich) was added to the medium and rEpiSCs were cultured for 3–4 days. After G418 selection, six transcription factors-transfected rEpiSCs (6TFs-rEpiSCs) were re-plated at 2–10 x 10e4 cells per well of MEF-coated 12-well plates containing 1 mL of rEpiSC medium supplemented with 1 μg/mL Dox (Sigma-Aldrich). The next day, the medium was replaced by rESC medium supplemented with Dox. The PV(+) dome-shaped colonies were picked manually at day 5–7 and then dissociated by 0.25% Trypsin-EDTA into single cells and re-plated into a well of 12-well plates containing 1 mL of rESC medium without Dox. PV(+) rESCLCs were routinely passaged every 3 days.

Quantitative reverse transcription PCR

Total RNA was extracted using PicoPure RNA Isolation Kit and cDNA was synthesized using QuantiTect Reverse Transcription Kit (QIAGEN, Venlo, The Netherland) according to the manufacturer's protocols. qRT-PCR were performed and analyzed as described previously,[56] and the primers sequences used in the paper are listed in Table S3.

Preparation of RNA-sequencing libraries

Total RNA was extracted using the PicoPure RNA Isolation Kit following the manufacturer's protocol. cDNA library was constructed using SMART-Seq HT PLUS Kit (Takara Bio) and following the manufacturer's recommendations. For Illumina sequencing, cDNA was synthesized from 1 ng of total RNA with 10 cycles of PCR amplification, subsequently, 5 ng of cDNA was used for the addition of Illumina's adaptors with 13 cycles of PCR amplification. The quality and quantity of RNA-seq libraries were evaluated by qPCR using KAPA Library Quantification Kit (Kapa Biosystems). All libraries were pooled and applied to single-end 86 bp sequencing on NexSeq 500 system (Illumina, San Diego, CA) using High Output Kit v2.5. Basecalls were performed using NextSeq 500/550 RTA software (v2.11.3). FASTQ files were generated using bcl2fastq (v2.17.1.14). Two technical replicates of all samples were used for the analysis. RNA-seq data had been deposited in the Gene Expression Omnibus (GEO) under accession number GSE220805.

Flow cytometry analysis

rPSCs including resetting cells and rPGCLCs were analyzed and sorted by SH800 cell sorter (SONY, Tokyo, Japan) or BD FACSAria III cell sorter (BD Biosciences, Franklin Lakes, NJ).

Immunofluorescence analysis

Samples were fixed with 4% paraformaldehyde for 10–30 min at an ambient temperature or from 4 h to overnight at 4°C. The fixed samples were treated with a gradient of 10%, 20%, and 30% sucrose solution and subsequently embedded in OCT compound for cryosectioning (Sakura Finetek, Tokyo, Japan). Samples were cut into 7 μm-thick cryosections using Cryostat (Leica Biosystems, Wetzlar, Germany) and then dried and washed with PBS and PBS/0.1% Triton X- each three times. After incubating with blocking buffer (5% normal donkey serum (Sigma-Aldrich), 1% BSA, 0.1% Triton X- in PBS) for 30 min, the sections were incubated with primary antibodies for 1–2 h. Next, the sections were washed three times with PBS/0.1% Triton X-, and were incubated with fluorescent-conjugated secondary antibodies with DAPI (Dojindo) for 1 h. After washing three times with PBS/0.1% Triton X-, samples were mounted with mounting medium. Antibodies used are listed on Table S4. Specimens were observed and analyzed using FV3000 (Olympus, Tokyo, Japan).

QUANTIFICATION AND STATISTICAL ANALYSIS

Flow cytometry analysis

FACS data were analyzed and visualized by Flowjo software (BD Biosciences).

Bioinformatics analysis

For processing the RNA-seq data, we used RaNA-seq program (https://ranaseq.eu/index.php) to calculate TPM values. For further analysis, rat genes showing maximum log2 (TPM+1) values > 4 in at least one replicate were selected (9606 genes). Hierarchical clustering was performed based on Ward's method using the 'htclust' function of R package. The PCA was performed using the 'tidyverse' function of the R package.

For cross-species comparison analysis, existing *in vitro* transcriptomic data from mouse ESC and EpiSC[10] (GSE131556), *in vivo* data from mouse E4.5-E7.5 embryo ref. 33 (GSE121650) were downloaded and trimmed using TrimGalore! (https://doi.org/10.5281/zenodo/7598955) and aligned to mouse genome mm10 using STAR aligner[51] (v2.5.4b).

For integrative analyses, *in vitro* datasets were merged using the Seurat merge function, and aligned to an *in vivo* reference dataset (GSE121650) using the Seurat v3.1.2[52] function FindIntegrationAnchors (2000 integration features, 20 PCs, 10 anchor features). Reduced dimensionality plots were generated using the runPCA/runUMAP functions. Correlations based on raw log2(CP10k + 1) and integration corrected expression matrices were calculated based on pseudobulk averages (using the Seurat Average Expression function and R cor function) and visualised using pheatmap (v1.0.12).

Statistical analysis

Quantitative data were generated with Microsoft Office Excel or GraphPad Prism and presented as means ± SD. All statistical details of the experiments can be found in the figure legends.